Intestinal Nogo-B reduces the GLP1 levels by binding to proglucagon on the endoplasmic reticulum to inhibit PCSK1 cleavage

SUPPLEMENTARY INFORMATION

This PDF file includes:

- **Supplementary Figures S1-S16**
- **Supplementary Tables S1-S6**
- **Uncropped Scans of Blots in Supplementary Figures**

Supplementary Figures:

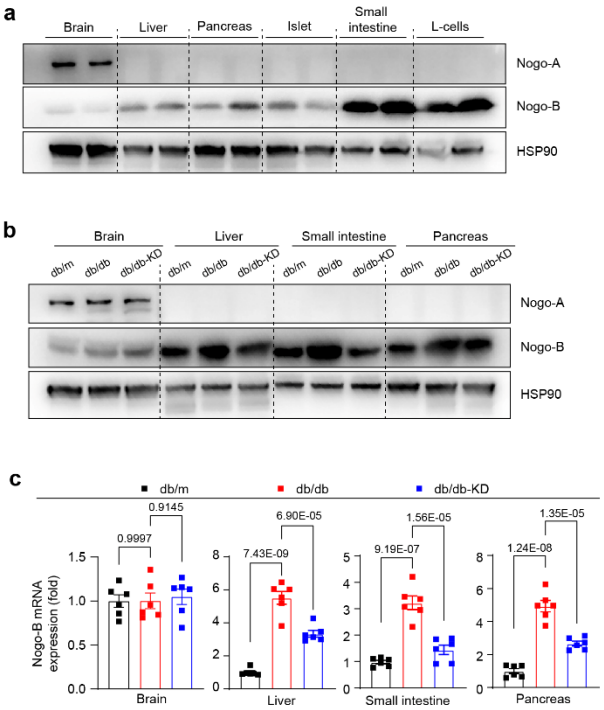

Supplementary Figure 1. The levels of Nogo-A and Nogo-B in different tissues of C57BL/6J mice and db/db mice. a, Nogo-A and Nogo-B protein levels in different tissues of C57BL/6J mice. **b, c**, Nogo-A and Nogo-B protein and mRNA levels in different tissues of db/db mice (n = 6 mice per group). Data are expressed as the mean ± SEM. The *p* values were calculated by one-way ANOVAs. Source data are provided as a Source Data file.

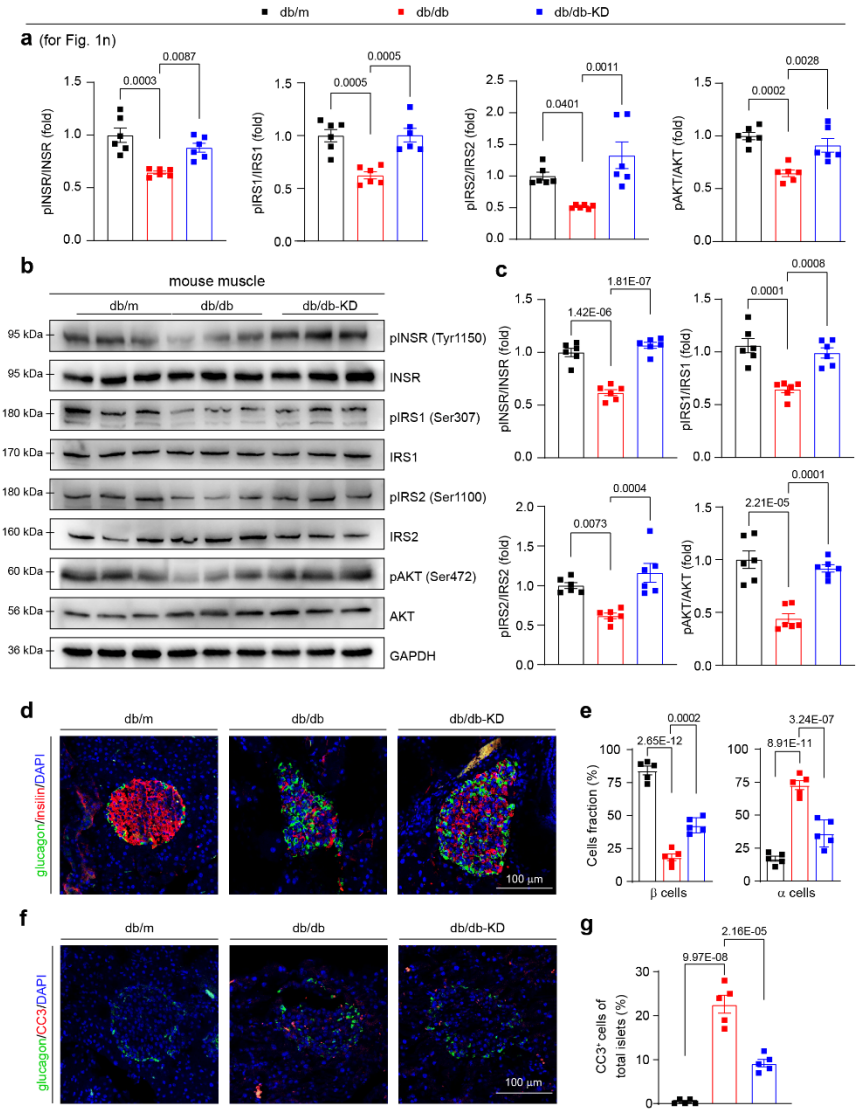

Supplementary Figure 2. Muscle insulin sensitivity and pancreatic injury of db/db mice. a, Analysis of band density in Fig. 1n (n = 6 mice per group). **b, c**, pINSR, INSR, pIRS1, IRS1, pIRS2, IRS2, pAKT and AKT protein levels in mouse muscle and analysis of band density (n = 6 mice per group). **d**, Islet images after siRNA injection (insulin, red; glucagon, green; DAPI, blue). **e**, Analysis of β-cell or α-cell as the percentage of pancreatic cells after siRNA injection (n = 5 mice per group). **f**, **g,** Islet images after siRNA injection (CC3, cleaved caspase 3, red; glucagon, green; DAPI, blue). Analysis of $CC3^+$ cells as the percentage of pancreatic cells after siRNA injection (n = 5 mice per group). Data are expressed as the mean ± SEM. The *p* values were calculated by one-way ANOVAs. Source data are provided as a Source Data file.

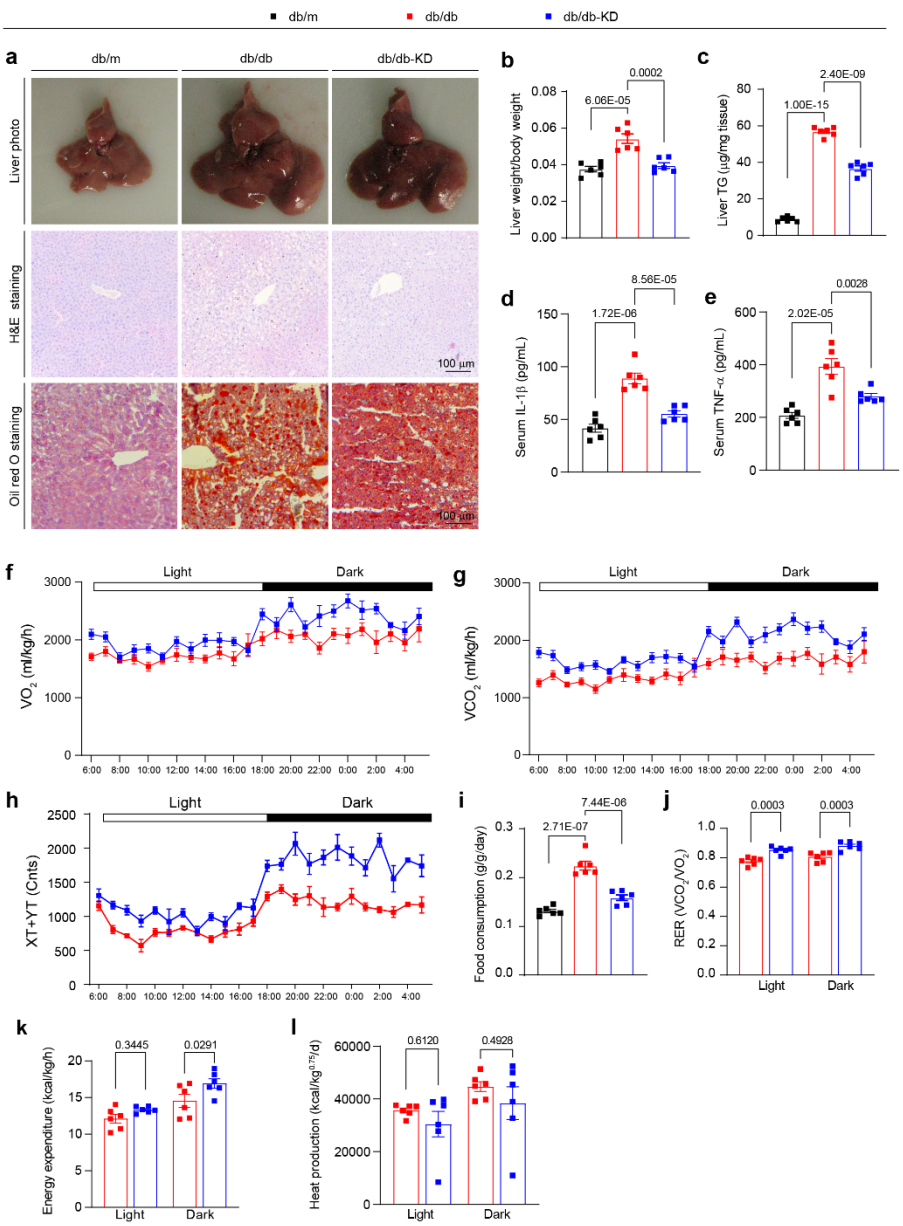

Supplementary Figure 3. Nogo-B knockdown reduced liver injury and lipid accumulation in db/db mice. a, Representative photographs of the whole liver, H&E and oil red O staining images of the liver sections of mice after siRNA injection. **b**, Liver weight to body weight of mice after siRNA injection (n= 6 mice per group). **c**, Liver TG levels of mice after siRNA injection (n = 6 mice per group). **d, e**, Serum IL-1β and TNF-α levels of mice (n = 6 mice per group). **f, g**, The curves of O2 consumption (**f**) and CO2 production (**g**) of mice after siRNA injection during a 24-h light–dark cycle (n= 6 mice per group). **h**, The locomotor activity of mice after siRNA injection during a 24-h light–dark cycle (n= 6). **i**, Food consumption of mice after siRNA injection (n= 6 mice per group). **j-l**, The respiratory exchange rate (RER) (**j**), energy expenditure (**k**), and heat production (**l**) of mice after siRNA injection (n = 6 mice per group). Data are expressed as the mean ± SEM. The *p* values were calculated by one-way ANOVAs. Source data are provided as a Source Data file.

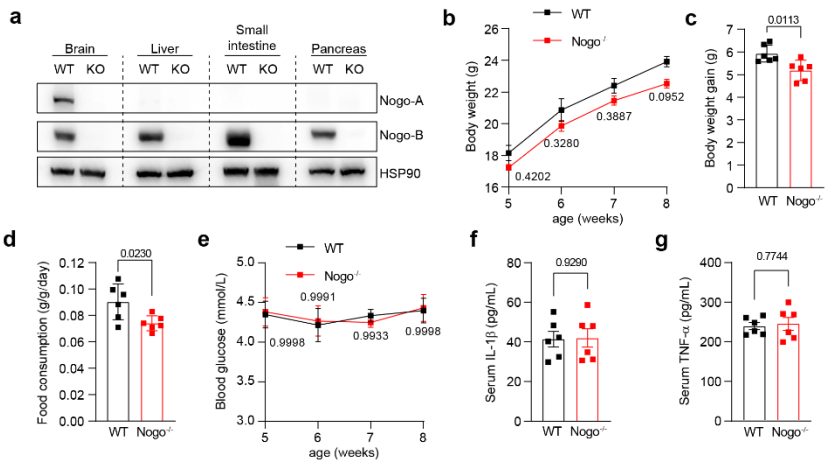

Supplementary Figure 4. Nogos levels and basal signs of Nogo$^{-/-}$ mice. a, Nogo-A and Nogo-B protein levels in different tissues of WT and Nogo$^{-/-}$ mice. **b**, Body weight of WT and Nogo$^{-/-}$ mice (n = 6 mice per group). **c**, Body weight gain of WT and Nogo$^{-/-}$ mice (n = 6 mice per group). **d**, Food consumption of WT and Nogo$^{-/-}$ mice (n = 6 mice per group). **e**, Fasted glucose levels of WT and Nogo$^{-/-}$ mice (n = 6 mice per group). **f, g,** Serum IL-1β and TNF-α levels of WT and Nogo$^{-/-}$ mice (n = 6 mice per group). Data are expressed as the mean ± SEM. The *p* values were calculated by two-tailed Student's t test. Source data are provided as a Source Data file.

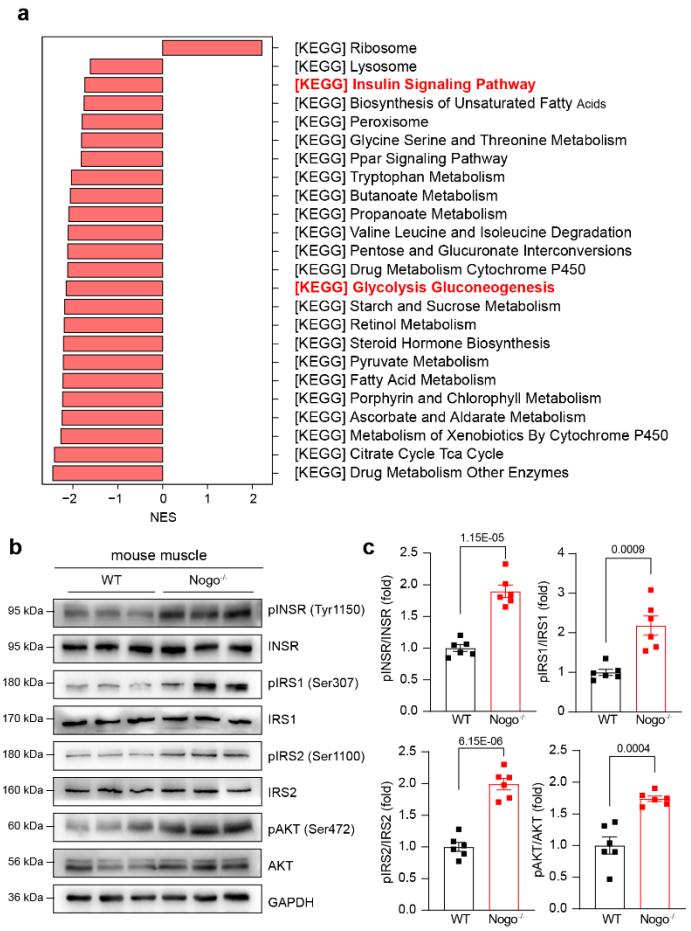

Supplementary Figure 5. Gene enrichment analysis (GSEA) and muscle insulin sensitivity WT and Nogo$^{-/-}$ mice. a, GSEA was performed to analyze the pathways affected by Nogo deficiency in the liver. **b, c**, pINSR, INSR, pIRS1, IRS1, pIRS2, IRS2, pAKT and AKT protein levels in mouse muscle and analysis of band density (n = 6 mice per group). Data are expressed as the mean ± SEM. The *p* values were calculated by two-tailed Student's t test. Source data are provided as a Source Data file.

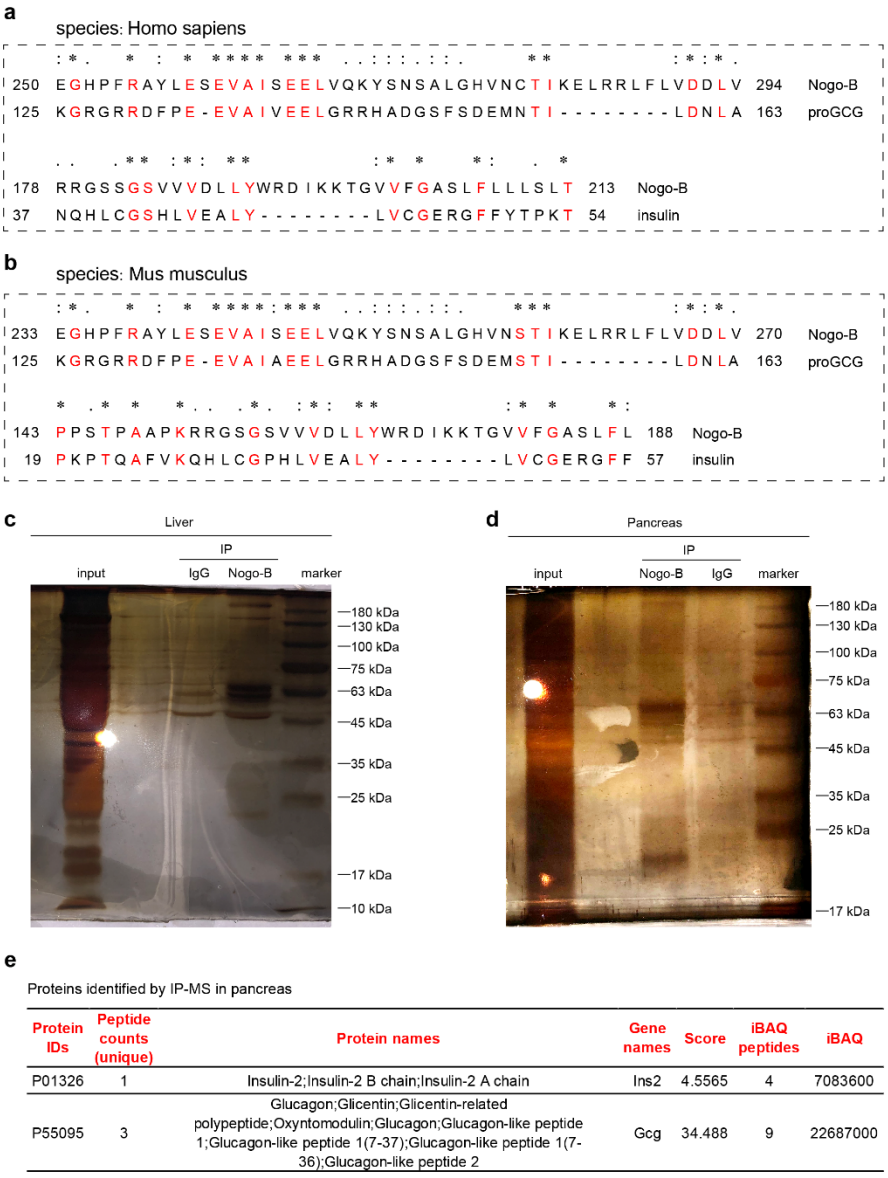

e

Proteins identified by IP-MS in pancreas

Protein IDs	Peptide counts (unique)	Protein names	Gene names	Score	iBAQ peptides	iBAQ
P01326	1	Insulin-2;Insulin-2 B chain;Insulin-2 A chain	Ins2	4.5565	4	7083600
P55095	3	Glucagon;Glicentin;Glicentin-related polypeptide;Oxyntomodulin;Glucagon;Glucagon-like peptide 1;Glucagon-like peptide 1(7-37);Glucagon-like peptide 1(7-36);Glucagon-like peptide 2	Gcg	34.488	9	22687000

Supplementary Figure 6. Immunoprecipitation-mass spectrometry (IP-MS) assays. a, b, Sequence comparisons between Nogo-B and proGCG or insulin in different species. **c, d,** IP-silver staining assays with a Nogo-B antibody using extracts from excised liver and pancreas samples from C57BL/6J mice. **e**, IP-MS results showed that Nogo-B interacts with insulin and proGCG in the pancreas.

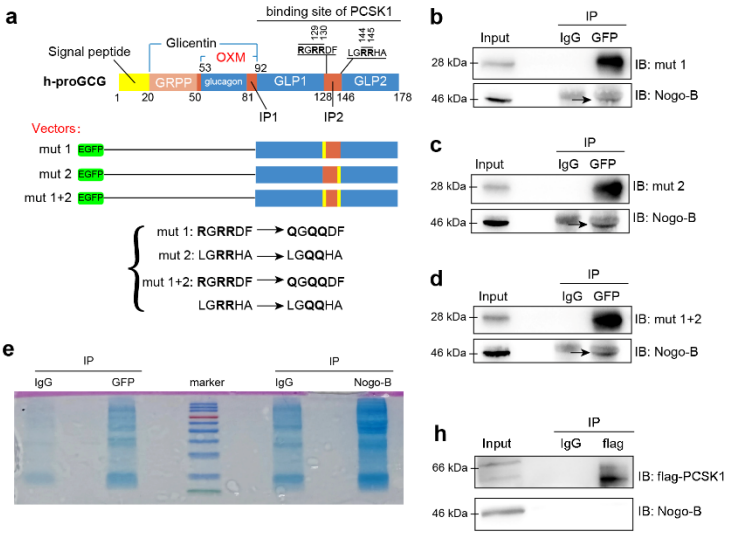

f

co-IP-MS using anti-Nogo-B antibody

the detected peptides of MPGF	position	score
K.EFIAWLVK.G	118-125	33.64
R.DFINWLIQTK.I	166-175	48.47
R.DFPEEVAIVEELGR.R	131-144	72.05
R.DFPEEVAIVEELGR.R	131-144	65.84
R.HADGSFSDEMNTILDNLAAR.D	146-165	89.34
R.HAEGTFTSDVSSYLEGQAAK.E	98-117	73.03
R.RDFPEEVAIVEELGR.R	130-144	53.07

g

co-IP-MS using anti-GFP antibody

The detected peptides of Nogo-B	position	score
K.GVIQAIQK.S	234-241	39.11
K.SDEGHPFR.A	241-248	39.18
K.SDEGHPFR.A	241-248	30.12
K.YQFVR.E	22-26	23.28
K.YSNSALGHVNCTIK.E	258-272	73.84
R.AYLESEVAISEELVQK.Y	241-256	88.15
R.GPLPAAPPVAPER.Q	80-92	57.47
R.GPLPAAPPVAPER.Q	80-92	53.49
R.HQAQIDHYLGLANK.N	326-339	35.39
R.HQAQIDHYLGLANK.N	326-339	75.98
R.KPAAGLSAAPVPTAPAAGAPLM&DFGNDFVPPAPR.G	25-58	90.81
R.KPAAGLSAAPVPTAPAAGAPLM&DFGNDFVPPAPR.G	25-58	31.26
R.KPAAGLSAAPVPTAPAAGAPLMDFGNDFVPPAPR.G	25-58	100.74
R.KPAAGLSAAPVPTAPAAGAPLMDFGNDFVPPAPR.G	25-58	74.21
R.LFLVDDLVDSLK.F ! R.LFLVDDLVDSLK.A	181-206	67.44
R.QPSWDPSPVSSTVPAPSPLSAAAVSPSK.L	88-105	85.84

Supplementary Figure 7. co-IP detection of peptide mutations in the PCSK1 binding site and co-IP-MS detection. a, Construction of EGFP-tagged expression vectors for MPGF with PCSK1 shear site mutations. **b-c**, Immunoprecipitation assay with Nogo-B and MPFG with PCSK1 shear site mutations (n = 3 biological replicates). **e**, co-IP products stained with Coomassie Brilliant Blue staining. **f**, proGCG peptide conjugated to Nogo-B obtained using Noog-B antibody (n = 3 biological replicates). **g**, Nogo-B peptide conjugated to proGCG obtained using GFP antibody. **h**, Immunoprecipitation assay with Nogo-B and PCSK1. Source data are provided as a Source Data file.

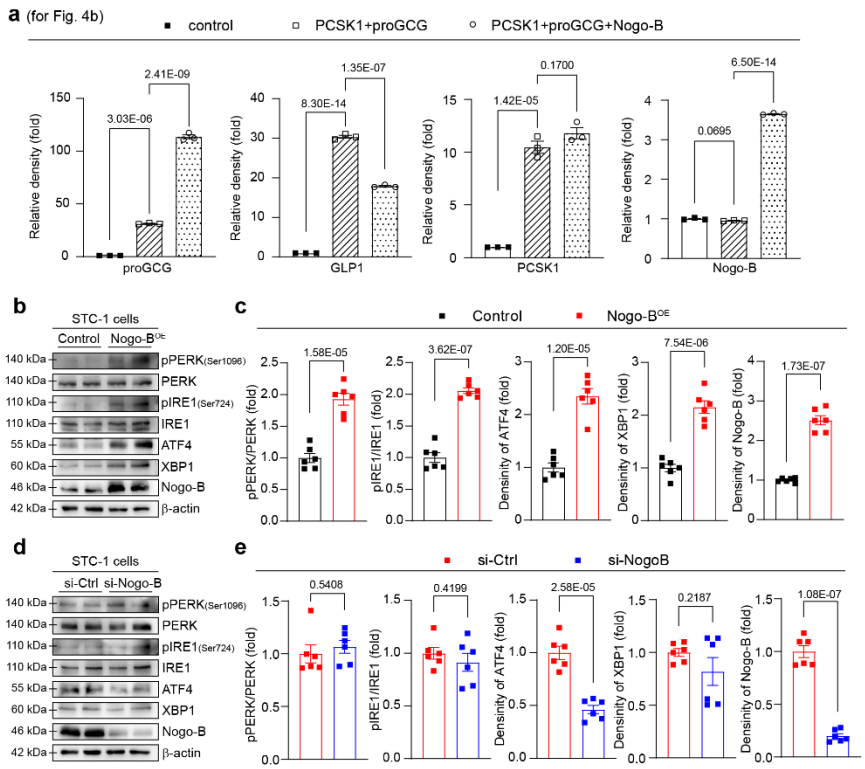

Supplementary Figure 8. Effect of Nogo-B expression on the UPR. a, Analysis of band density in Fig. 4b (n = 3 biological replicates). **b-e**, Effect of Nogo-B expression on protein levels of pPERK, PERK, pIRE1, IRE1, ATF4, and XBP1 and analysis of band density. (n = 6 biological replicates)). Data are expressed as the mean ± SEM. The *p* values were calculated by two-tailed Student's t test. Source data are provided as a Source Data file.

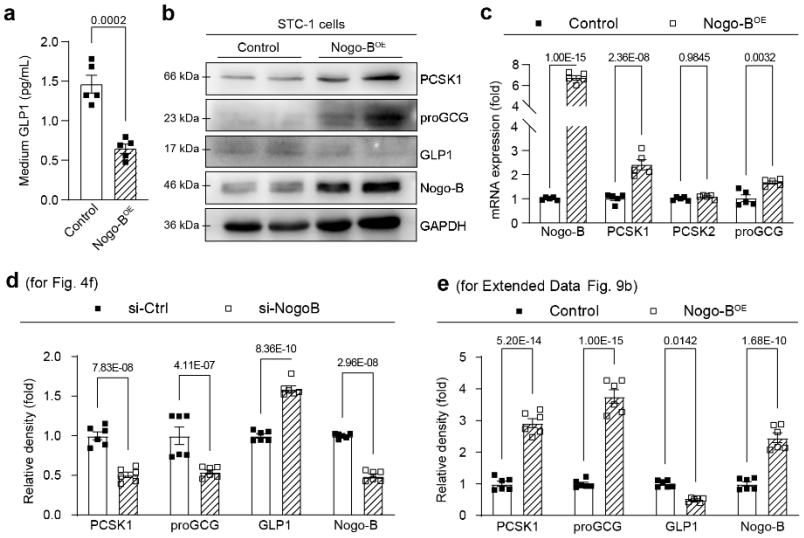

Supplementary Figure 9. Effect of Nogo-B overexpression on GLP1 levels in STC-1 cells. a, GLP1 levels in the culture medium of STC-1 cells transfected with empty vector (Control) or Nogo-B expression vector (Nogo-B^{OE}) (n = 5 biological replicates). **b**, PCSK1, proGCG, GLP1 and Nogo-B protein levels in STC-1 cells transfected with Control or Nogo-B^{OE} vector (n = 6 biological replicates). **c**, Nogo-B, PCSK1, PCSK2 and proGCG mRNA levels in STC-1 cells transfected with Control or Nogo-B^{OE} vector (n = 5 biological replicates). **d, e**, Analysis of band density in Fig. 4f and Supplementary Figure 9b (n = 6 biological replicates) Data are expressed as the mean ± SEM. The *p* values were calculated by two-tailed Student's t test. Source data are provided as a Source Data file.

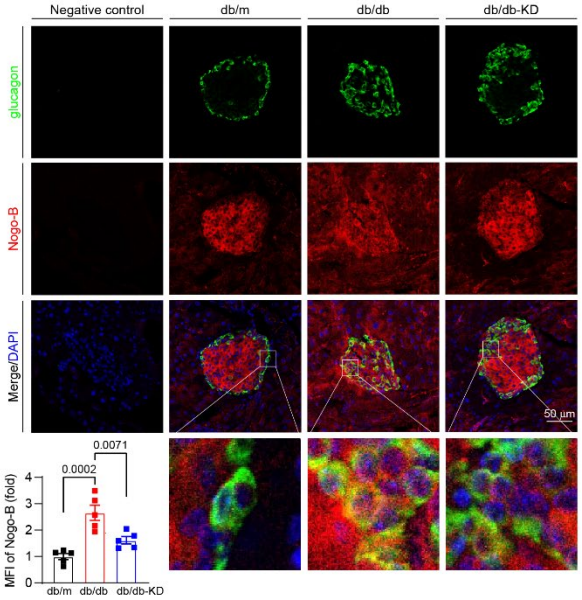

Supplementary Figure 10. Localization and expression of Nogo-B in pancreas. Representative images of immunofluorescence staining (glucagon, green; Nogo-B, red; DAPI, blue) of pancreas from db/m, db/db, and db/db-KD mice (n = 5 biological replicates)**.** Data are expressed as the mean ± SEM. The *p* values were calculated by one-way ANOVAs. Source data are provided as a Source Data file.

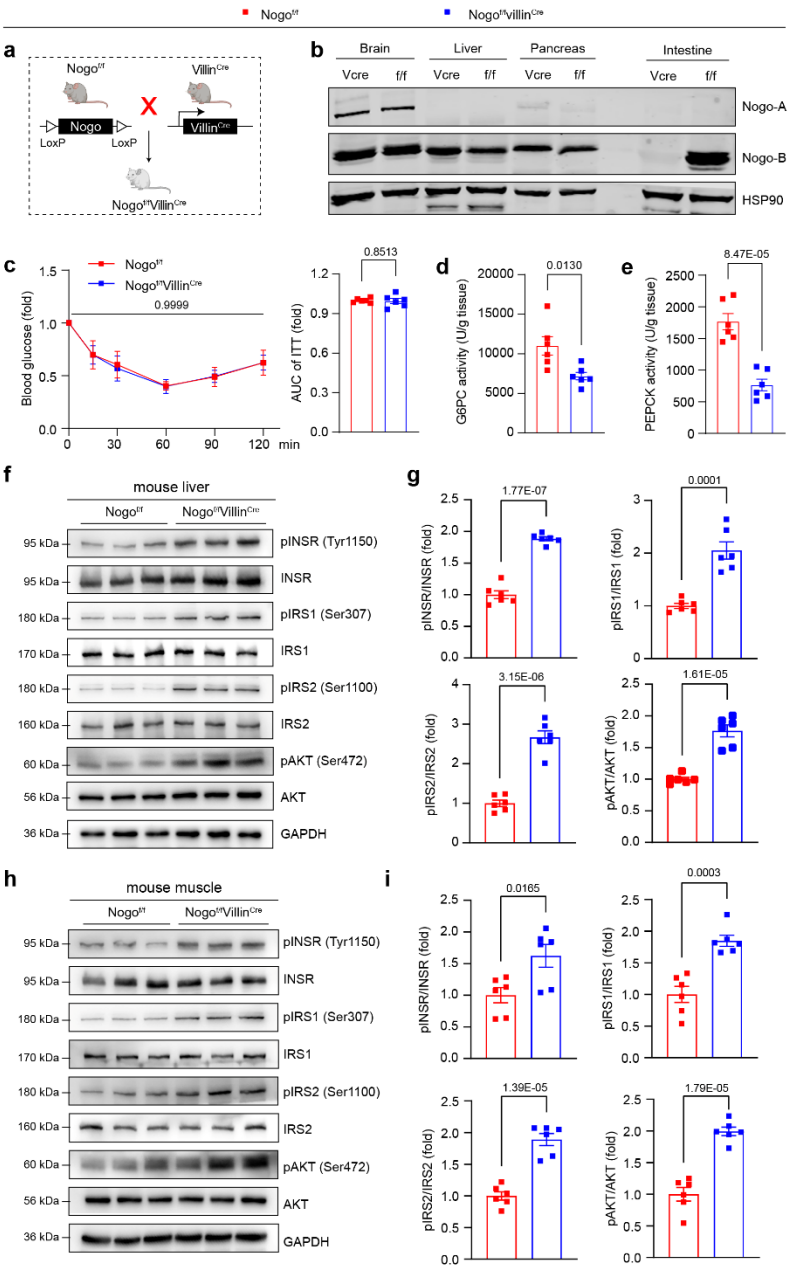

Supplementary Figure 11. Intestinal Nogo-B knockout increases insulin sensitivity in mice. **a**, A strategy for generating intestinal Nogo-selectively knockout mice ($Nogo^{f/f}Villin^{Cre}$). **b**, Validation of intestinal Nogo-B-selectively knockout in mice by Western blotting. **c**, ITT and AUC analysis of mice (n = 6 mice per group). **d, e**, The enzyme activity of G6PC (**d**) and PEPCK (**e**) in the liver of $Nogo^{f/f}Villin^{Cre}$ and $Nogo^{f/f}$ mice (n = 6 mice per group). **f-i**, pINSR, INSR, pIRS1, IRS1, pIRS2, IRS2, pAKT and AKT protein levels in mouse liver and muscle and analysis of band density (n = 6 mice per group). Data are expressed as the mean ± SEM. The *p* values were calculated by two-tailed Student's t test. Source data are provided as a Source Data file.

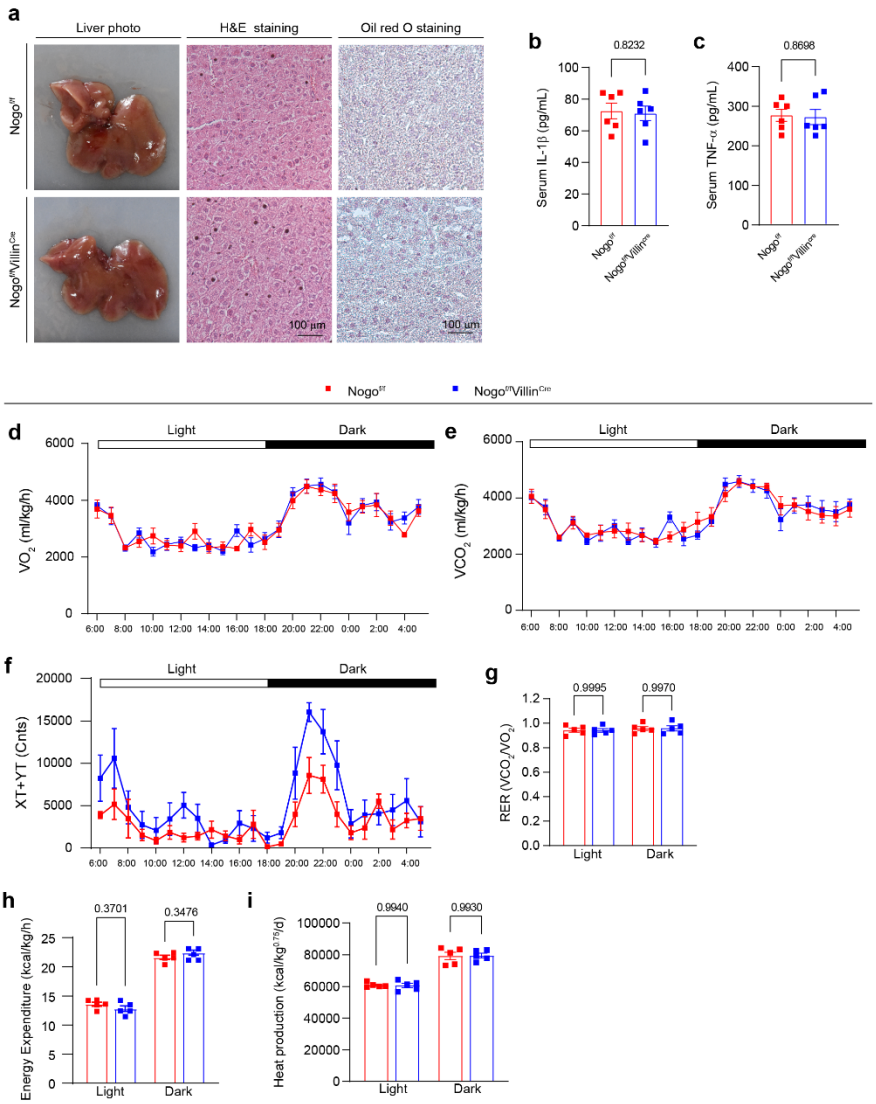

Supplementary Figure 12. Intestinal Nogo-B knockout does not affect liver function and metabolism in mice. a, Representative photographs of the whole liver, H&E and oil red O staining images of the liver sections of Nogo$^{f/f}$Villin^{Cre} and Nogo$^{f/f}$ mice. **b, c**, Serum IL-1β and TNF-α levels of Nogo$^{f/f}$Villin^{Cre} and Nogo$^{f/f}$ mice (n = 6 mice per group). **d, e**, The curves of O2 consumption (**d**) and CO2 production (**e**) of Nogo$^{f/f}$Villin^{Cre} and Nogo$^{f/f}$ mice (n = 5). **f**, The locomotor activity of Nogo$^{f/f}$Villin^{Cre} and Nogo$^{f/f}$ mice (n = 5 mice per group). **g-i**, The RER, energy expenditure, and heat production of Nogo$^{f/f}$Villin^{Cre} and Nogo$^{f/f}$ mice (n = 5 mice per group). Data are expressed as the mean ± SEM. The *p* values were calculated by two-tailed Student's t test. Source data are provided as a Source Data file.

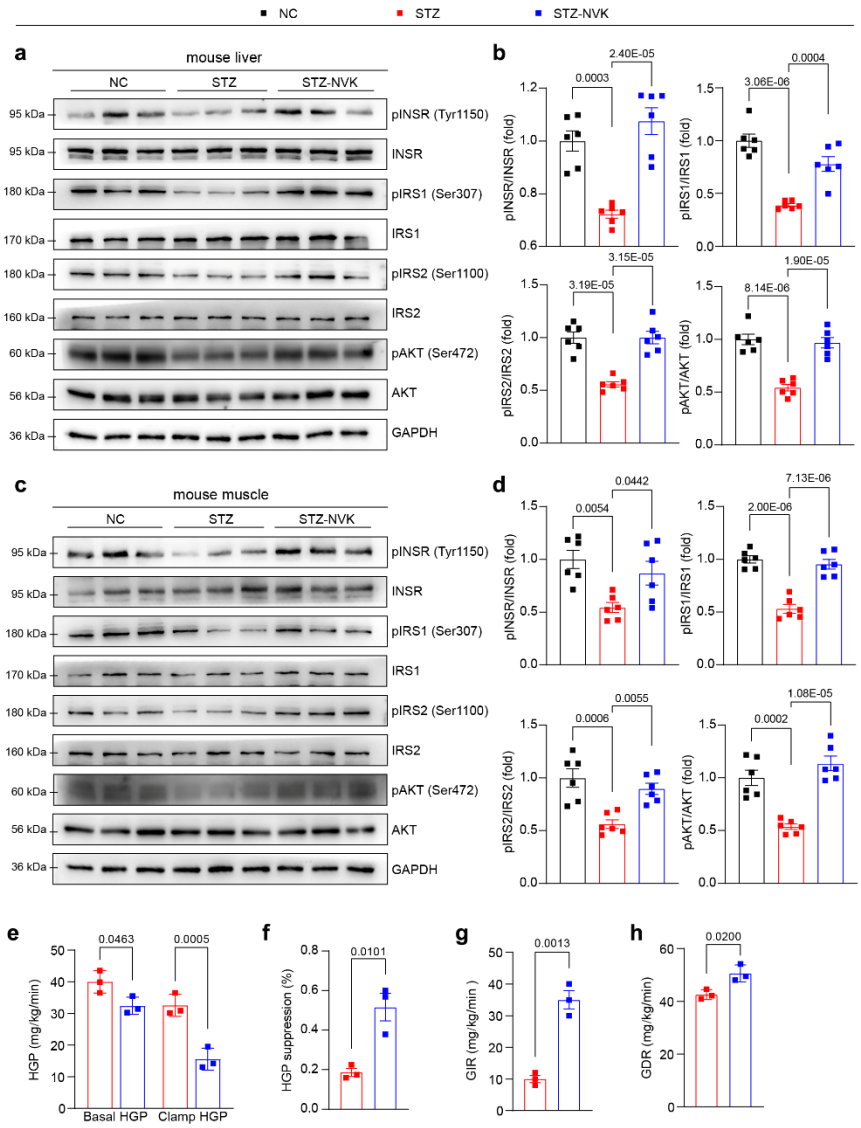

Supplementary Figure 13. Intestinal Nogo-B knockout improved insulin sensitivity in STZ-induced T2DM mice. a-d, pINSR, INSR, pIRS1, IRS1, pIRS2, IRS2, pAKT and AKT protein levels in mouse liver and muscle and analysis of band density (n = 6 mice per group). **e**, HGP under basal and clamp conditions of mice (n = 3 mice per group). **f-h**, HGP suppression (**f**), glucose infusion rate GIR (**g**) ,and GDR (**h**) of mice (n = 3 mice per group). Data are expressed as the mean ± SEM. The *p* values of (**b, d**) were calculated by one-way ANOVAs. The *p* values of (**e-h**) were calculated by two-tailed Student's t-test. Source data are provided as a Source Data file.

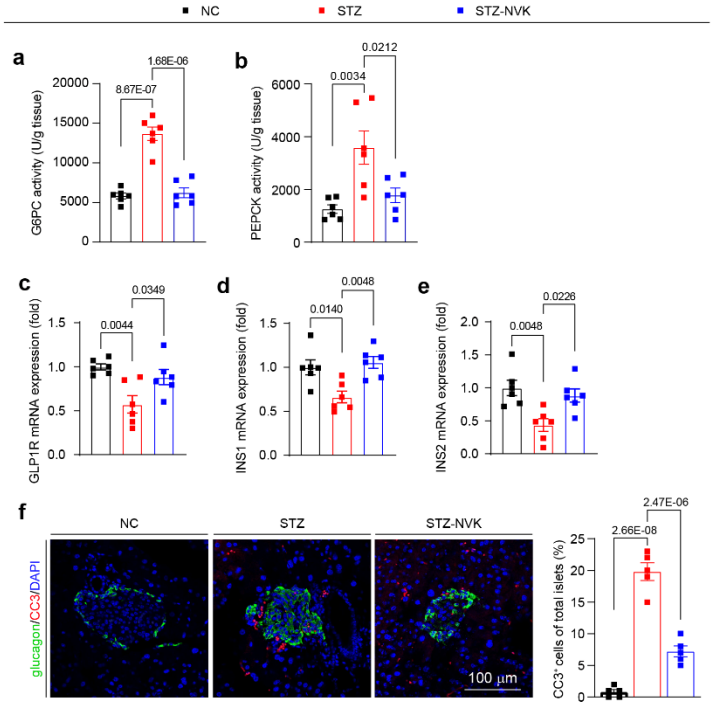

Supplementary Figure 14. Intestinal Nogo-B knockout recovered STZ-induced T2DM symptom. a, b, The enzyme activity of G6PC (**a**) and PEPCK (**b**) in the liver of mice in NC, STZ, and STZ-NVK groups (n = 6 mice per group). **c-e**, The mRNA levels of GLP1R, INS1, and INS2 in the pancreas of mice in NC, STZ, and STZ-NVK groups (n = 6 mice per group). **e**, Islet images of mice in NC, STZ, and STZ-NVK groups (CC3, caspase 3, red; glucagon, green; DAPI, blue) and analysis of $CC3^+$ cells as the percentage of pancreatic cells after siRNA injection (n = 6 mice per group). Data are expressed as the mean ± SEM. The *p* values of were calculated by one-way ANOVAs. Source data are provided as a Source Data file.

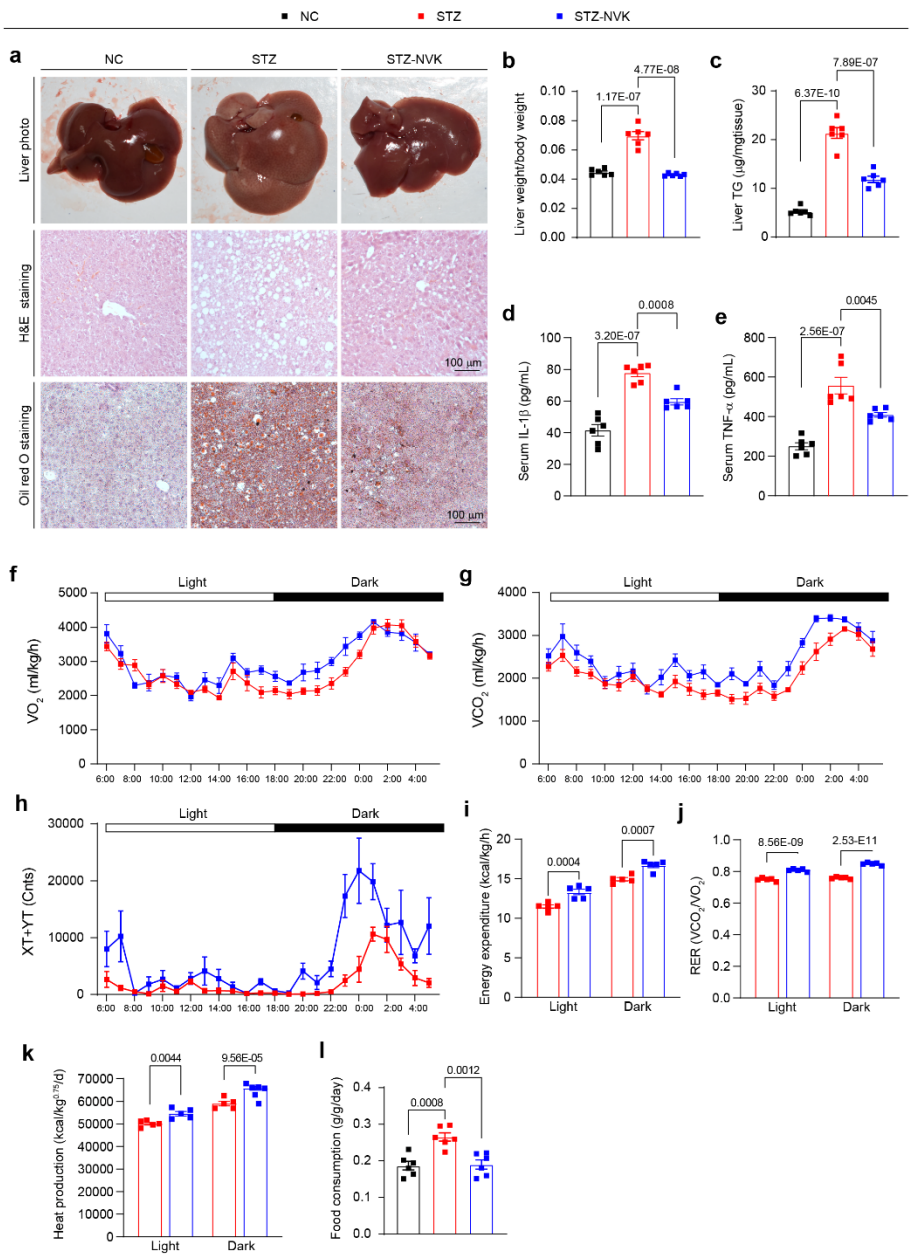

Supplementary Figure 15. Intestinal Nogo-B knockout reduced liver injury and lipid accumulation in mice with T2DM induced by STZ. a, Representative photographs of the whole liver, H&E and oil red O staining images of mice in NC, STZ, and STZ-NVK groups. **b**, Liver weight to body weight of mice in NC, STZ, and STZ-NVK groups (n = 6 mice per group). **c**, Liver TG levels of mice in NC, STZ, and STZ-NVK groups (n = 6 mice per group). **d, e**, Serum IL-1β and TNF-α levels of mice in NC, STZ, and STZ-NVK groups (n = 6 mice per group). **f, g**, The curves of O2 consumption (**f**) and CO2 production (**g**) of mice in NC, STZ, and STZ-NVK groups (n = 5 mice per group). **h**, The locomotor activity of mice in NC, STZ, and STZ-NVK groups (n = 5 mice per group). **I-k**, The RER, energy expenditure, and heat production of mice in NC, STZ, and STZ-NVK groups (n = 5 mice per group). **l**, Food consumption of mice in NC, STZ, and STZ-NVK groups (n = 6 mice per group). Data are expressed as the mean ± SEM. The *p* values were calculated by one-way ANOVAs. Source data are provided as a Source Data file.

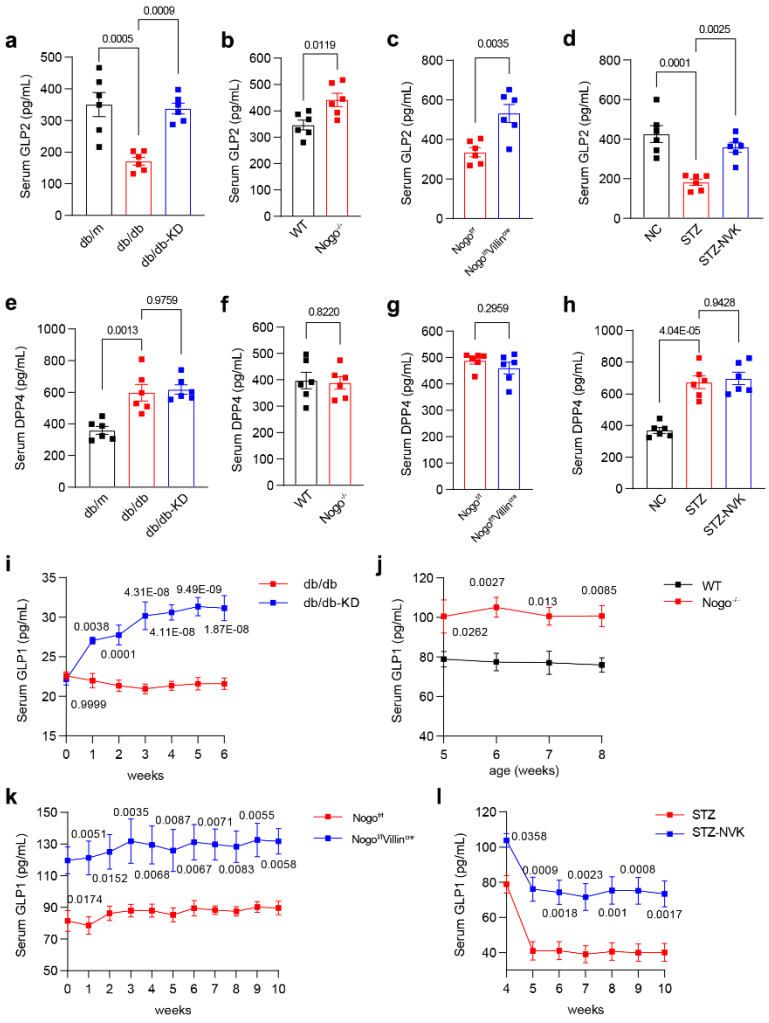

Supplementary Figure 16. Effect of Nogo-B expression on GLP2, DPP4 and weekly GLP1 levels. a-d, Effect of Nogo-B expression on serum GLP2 levels (n = 6 mice per group). **e-h**, Effect of Nogo-B expression on serum DPP4 levels (n = 6 mice per group). **i-l**, Effect of Nogo-B expression on weekly serum GLP1 levels. (n = 6 mice per group). Data are expressed as the mean ± SEM. The *p* values of (**a-d, i-l**) were calculated by one-way ANOVAs. The *p* values of (**e-h**) were calculated by two-tailed Student's t-test. Source data are provided as a Source Data file.

Supplementary Tables:

Table S1. siRNA-mediated knockdown of Nogo-B ameliorates hyperlipidemia and liver injury in db/db mice

	db/m	db/db	*p* (db/m *vs.* db/db)	db/db-KD	*p* (db/db *vs.* db/db-KD)
Triglyceride (mmol/L)	1.19 ± 0.22	4.02 ± 0.41	2.69E-07	2.09 ± 0.21	0.0004
Cholesterol (mmol/L)	2.81 ± 0.38	3.26 ± 0.26	0.4963	3.14 ± 0.16	0.9388
LDL-C (mmol/L)	0.21 ± 0.03	0.32 ± 0.03	0.1148	0.34 ± 0.04	0.9539
HDL-C (mmol/L)	2.35 ± 0.05	1.17 ± 0.13	4.89E-07	1.67 ± 0.07	0.0044
ALT (U/L)	38.1 ± 4.1	127 ± 10.8	1.90E-05	88.1 ± 11.3	0.0255
AST (U/L)	188.5 ± 21.5	244.6 ± 9.4	0.0866	199.8 ± 18.5	0.1905
ALP (U/L)	53.4 ± 1.8	101 ± 4.3	4.80E-07	72.6 ± 4.4	0.0002

The results are expressed as means ± SEM, the *p* values were calculated by one-way ANOVAs (n=6 mice per group).

Table S2. Intestinal Nogo knockout has no effect on blood lipid and transaminase levels in mice fed a high-glucose diet

	$Nogo^{f/f}$	$Nogo^{f/f}Villin^{Cre}$	*p* ($Nogo^{f/f}$ *vs.* $Nogo^{f/f}Villin^{Cre}$)
Triglyceride (mmol/L)	1.12 ± 0.05	1.21 ± 0.05	0.2319
Cholesterol (mmol/L)	4.14 ± 0.38	4.48 ± 0.44	0.621
LDL-C (mmol/L)	0.38 ± 0.04	0.39 ± 0.01	0.8946
HDL-C (mmol/L)	1.8 ± 0.06	1.77 ± 0.16	0.8571
ALT (U/L)	81.12 ± 5.1	75.96 ± 2.76	0.449
AST (U/L)	251.04 ± 7.6	264.3 ± 49	0.8172
ALP (U/L)	76.02 ± 3.3	74.64 ± 1.6	0.7443

The results are expressed as means ± SEM, the *p* values were calculated by two-tailed Student's t test (n=6 mice per group).

Table S3 Intestinal Nogo knockout ameliorates hyperlipidemia and liver injury in STZ-induced T2DM mice

	NC	STZ	*p* (NC *vs.* STZ)	STZ-NVK	*p* (STZ *vs.* STZ-NVK)
Triglyceride (mmol/L)	3.5 ± 0.12	5.92 ± 0.29	1.27E-06	4.15 ± 0.06	5.05E-05
Cholesterol (mmol/L)	2.75 ± 0.1	6.33 ± 0.37	2.25E-07	4.51 ± 0.16	0.0006
LDL-C (mmol/L)	0.3 ± 0.01	0.92 ± 0.08	1.04E-06	0.49 ± 0.02	7.78E-05
HDL-C (mmol/L)	1.26 ± 0.07	2.04 ± 0.12	0.0003	1.97 ± 0.11	0.8748
ALT (U/L)	80.9 ± 0.9	236.7 ± 12.9	1.02E-07	94.96 ± 11	3.50E-07

AST (U/L)	160.9 ± 15.9	295.7 ± 18.4	0.0002	206.2 ± 14.2	0.0077
ALP (U/L)	103.8 ± 7.2	131.8 ± 6.5	0.0271	102.1 ± 4.7	0.0194

The results are expressed as means ± SEM, the *p* values were calculated by one-way ANOVAs (n=6 mice per group).

Table S4. Sequences of the primers for qPCR and siRNA.

Gene	Forward	Reward
Species: mus		
FBP1	GGATATCAGCACCCTGACCC	AGCGATACCATAGAGCTGTGC
G6PC	AGACTCCCAGGACTGGTTCA	CTGCCACCCAGAGGAGATTG
GAPDH	TGTTTCCTCGTCCCGTAG	CAATCTCCACTTTGCCACT
GCK	TGAGCCGGATGCAGAAGGA	GCAACATCTTTACACTGGCCT
GLP1R	TTCACTTCCTTCCAGGGCTTG	CTGCTGGTGGGACACTTGAG
HK	GGCAAACATCCATTCTGTGACT	AGCGGGGTTTTCTGATCCTTGA
INS1	GGGCCAAACAGCAAAGTCCA	CCATGTTGAAACAATGACCTGC
INS2	CAGCAAGCAGGAAGGTTATTGT	CAGGTGGGAACCACAAAGGT
LDH	AACTTGGCGCTCTACTTGCT	GGACTTTGAATCTTTTGAGACCTTG
Nogo-B	TCGGGCTCAGTGGTTGTT	GAGACAGCAGCAGGAATAAGCT
PCK1	CTGCATAACGGTCTGGACTTC	CAGCAACTGCCCGTACTCC
PCSK1	CTTTCGCCTTCTTTTGCGTTT	TCCGCCGCCCATTCATTAAC
PCSK2	AGAGAGACCCCAGGATAAAGATG	CTTGCCCAGTGTTGAACAGGT
PFKL	ATTCATTCCTGAAGCGCCCC	CTGTGGTTCTGGAGGCATCCTT
PK	TATCGCAGCAGGAACCGAAG	GCATGGTTCCTGAAGTCCTTTG
proGCG	TTACTTTGTGGCTGGATTGCTT	AGTGGCGTTTGTCTTCATTCA
siRNA	**sense**	**antisense**
si-Ctrl	5’-UUCUCCGAACGUGUCACGUdTdT-3’	5’-ACGUGACACGUUCGGAGAAdTdT-3’
si-Nogo-B #1	5’-GGAUCUCAUUGUAGUCAUATT-3’	5’-UAUGACUACAAUGAGAUCCTT-3’
si-Nogo-B #2	5’-GCAGUGUUGAUGUGGGUAUUUTT-3’	5’-AAAUACCCACAUCAACACUGCTT-3’
si-Nogo-B #3	5’-CACAUAAACUAGGAAGAGATT-3’	5’-UCUCUUCCUAGUUUAUGUGTT-3’

Table S5. Sequences of the Recombinant DNA

peptides	Oligonucleotides
h-Nogo-B	NM_153828.3:152-1273 Homo sapiens reticulon 4
h-proGCG	NM_002054.5:100-642 Homo sapiens glucagon
h-insulin	NM_000207.3:60-392 Homo sapiens insulin
h-PCSK1	NM_000439.5:207-2468 Homo sapiens proprotein convertase subtilisin/kexin type 1

h-GRPP	ATGCGTTCCCTTCAAGACACAGAGGAGAAATCCAGATCATTCTCAGCTTCCCAGGCAGACCC ACTCAGTGATCCTGATCAGATGAACGAGGAC
h-GCG	ATGCATTCACAGGGCACATTCACCAGTGACTACAGCAAGTATCTGGACTCCAGGCGTGCCCA AGATTTTGTGCAGTGGTTGATGAATACC
h-GLP1	ATGCACGATGAATTTGAGAGACATGCTGAAGGGACCTTTACCAGTGATGTAAGTTCTTATTTGG AAGGCCAAGCTGCCAAGGAATTCATTGCTTGGCTGGTGAAAGGCCGAGGA
h-GLP2	ATGCATGCTGATGGTTCTTTCTCTGATGAGATGAACACCATTCTTGATAATCTTGCCGCCAGGG ACTTTATAAACTGGTTGATTCAGACCAAAATCACTGAC
h-GLI	ATGAAAAGCATTTACTTTGTGGCTGGATTATTTGTAATGCTGGTACAAGGCAGCTGGCAACGTT CCCTTCAAGACACAGAGGAGAAATCCAGATCATTCTCAGCTTCCCAGGCAGACCCACTCAGT GATCCTGATCAGATGAACGAGGACAAGCGCCATTCACAGGGCACATTCACCAGTGACTACAG CAAGTATCTGGACTCCAGGCGTGCCCAAGATTTTGTGCAGTGGTTGATGAATACCAAGAGGAA CAGGAATAACATTGCCAAACGT
h-MPGF	ATGCACGATGAATTTGAGAGACATGCTGAAGGGACCTTTACCAGTGATGTAAGTTCTTATTTGG AAGGCCAAGCTGCCAAGGAATTCATTGCTTGGCTGGTGAAAGGCCGAGGAAGGCGAGATTT CCCAGAAGAGGTCGCCATTGTTGAAGAACTTGGCCGCAGACATGCTGATGGTTCTTTCTCTG ATGAGATGAACACCATTCTTGATAATCTTGCCGCCAGGGACTTTATAAACTGGTTGATTCAGAC CAAAATCACTGAC
mut1	ATGCACGATGAATTTGAGAGACATGCTGAAGGGACCTTTACCAGTGATGTAAGTTCTTATTTGG AAGGCCAAGCTGCCAAGGAATTCATTGCTTGGCTGGTGAAAGGCCAAGGACAGCAAGATTTC CCAGAAGAGGTCGCCATTGTTGAAGAACTTGGCCGCAGACATGCTGATGGTTCTTTCTCTGAT GAGATGAACACCATTCTTGATAATCTTGCCGCCAGGGACTTTATAAACTGGTTGATTCAGACCA AAATCACTGAC
mut2	ATGCACGATGAATTTGAGAGACATGCTGAAGGGACCTTTACCAGTGATGTAAGTTCTTATTTGG AAGGCCAAGCTGCCAAGGAATTCATTGCTTGGCTGGTGAAAGGCCGAGGAAGGCGAGATTT CCCAGAAGAGGTCGCCATTGTTGAAGAACTTGGCCAACAGCATGCTGATGGTTCTTTCTCTG ATGAGATGAACACCATTCTTGATAATCTTGCCGCCAGGGACTTTATAAACTGGTTGATTCAGAC CAAAATCACTGAC
mut1+mut2	ATGCACGATGAATTTGAGAGACATGCTGAAGGGACCTTTACCAGTGATGTAAGTTCTTATTTGG AAGGCCAAGCTGCCAAGGAATTCATTGCTTGGCTGGTGAAAGGCCAAGGACAGCAAGATTTC CCAGAAGAGGTCGCCATTGTTGAAGAACTTGGCCAACAGCATGCTGATGGTTCTTTCTCTGAT GAGATGAACACCATTCTTGATAATCTTGCCGCCAGGGACTTTATAAACTGGTTGATTCAGACCA AAATCACTGAC
mut-F	ATGCACGATGAATTTGAGAGACATGCTGAAGGGACCTTTACCAGTGATGTAAGTTCTTATTTGG AAGGCCAAGCTGCCAAGGAATTCATTGCTTGGCTGGTGAAAGGCCGAGGAAGGCGAGATGC CCCAGAAGAGGTCGCCATTGTTGAAGAACTTGGCCGCAGACATGCTGATGGTTCTTTCTCTG ATGAGATGAACACCATTCTTGATAATCTTGCCGCCAGGGACTTTATAAACTGGTTGATTCAGAC CAAAATCACTGAC
mut-E	ATGCACGATGAATTTGAGAGACATGCTGAAGGGACCTTTACCAGTGATGTAAGTTCTTATTTGG AAGGCCAAGCTGCCAAGGAATTCATTGCTTGGCTGGTGAAAGGCCGAGGAAGGCGAGATTT

	CCCAGCCGCCGTCGCCATTGTTGCCGCCCTTGGCCGCAGACATGCTGATGGTTCTTTCTCTG ATGAGATGAACACCATTCTTGATAATCTTGCCGCCAGGGACTTTATAAACTGGTTGATTCAGAC CAAAATCACTGAC
mut-L	ATGCACGATGAATTTGAGAGACATGCTGAAGGGACCTTTACCAGTGATGTAAGTTCTTATTTGG AAGGCCAAGCTGCCAAGGAATTCATTGCTTGGCTGGTGAAAGGCCGAGGAAGGCGAGATTT CCCAGAAGAGGTCGCCATTGTTGAAGAAGCCGGCCGCAGACATGCTGATGGTTCTTTCTCTG ATGAGATGAACACCATTCTTGATAATCTTGCCGCCAGGGACTTTATAAACTGGTTGATTCAGAC CAAAATCACTGAC

Table S6. The characteristic of patients.

	No.	**Gender**	**Blood glucose (mmol/L)**
without T2DM	1	female	5.64
	2	female	5.46
	3	male	4.8
	4	male	4.61
	5	female	6.12
with T2DM	6	female	7.12
	7	female	19.46
	8	female	5.59
	9	male	8.24
	10	male	9.03

Figure 1n:

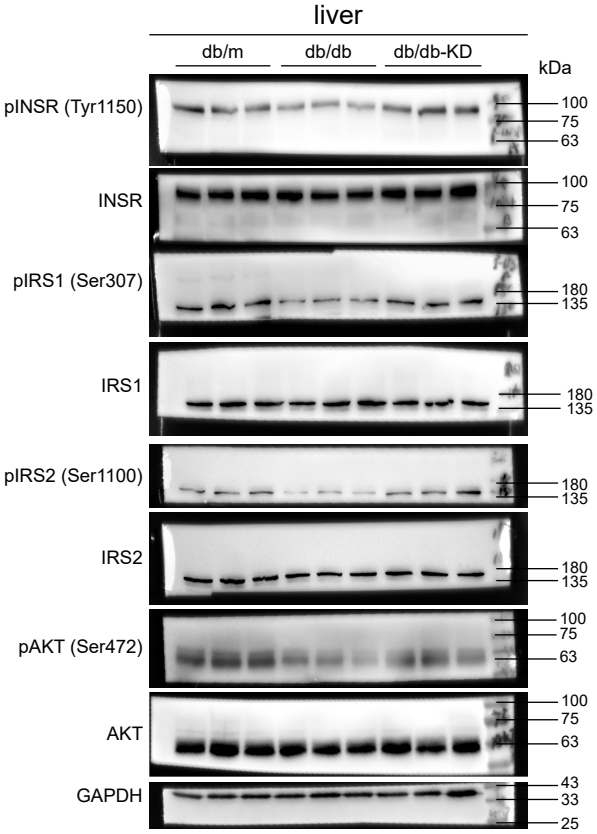

Figure 2j:

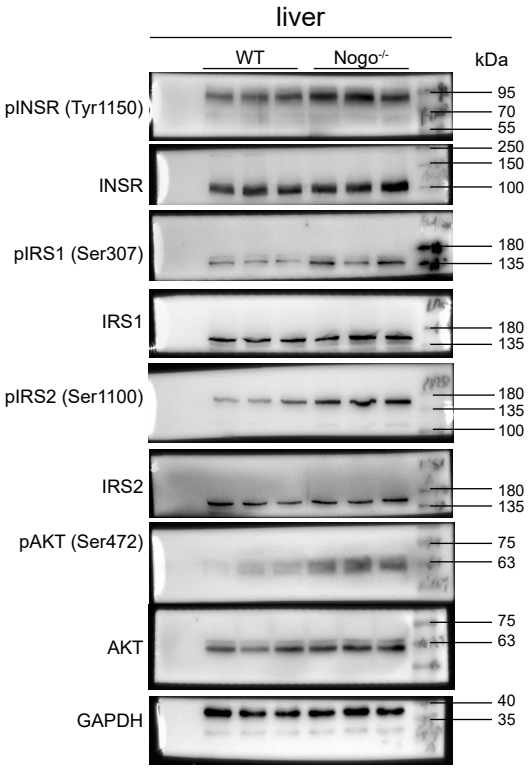

Figure 3b:

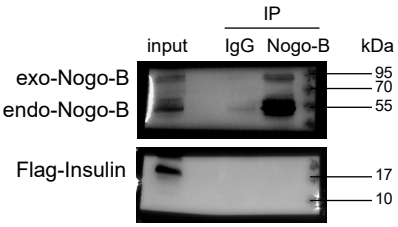

Figure 3c:

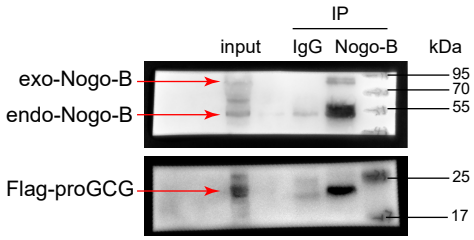

Figure 3d:

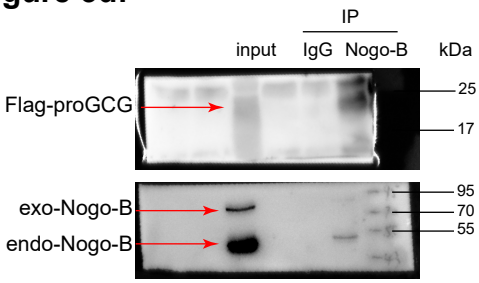

Figure 3f:

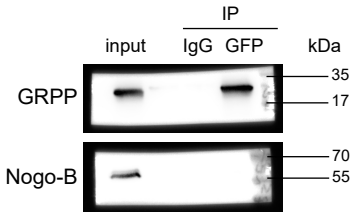

Figure 3g:

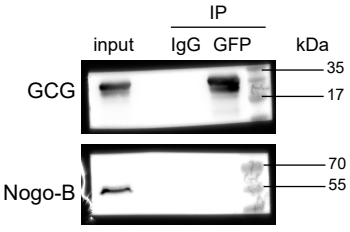

Figure 3h:

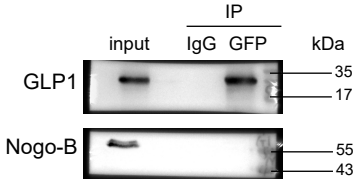

Figure 3i:

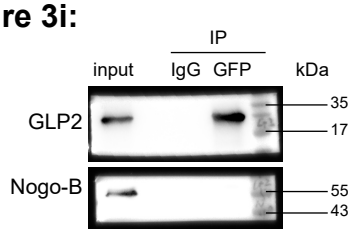

Figure 3k:

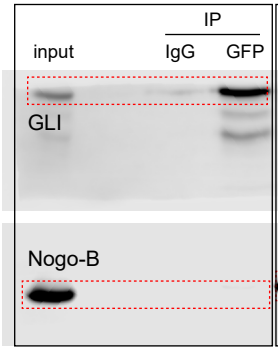

Figure 3l:

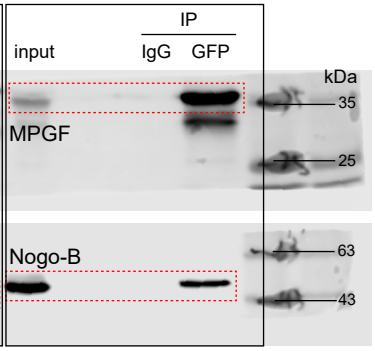

Figure 3n:

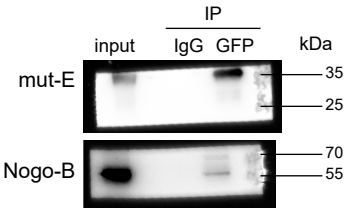

Figure 3o:

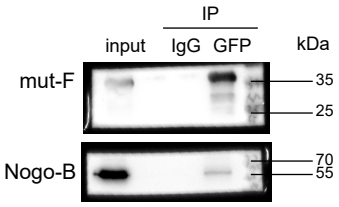

Figure 3p:

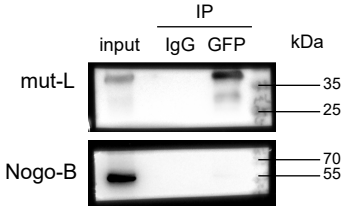

Figure 4b:

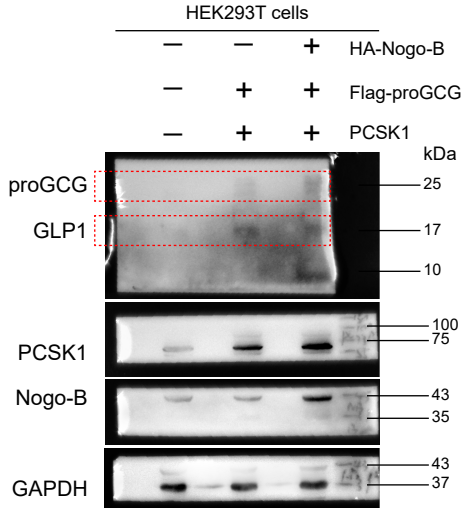

Figure 4c:

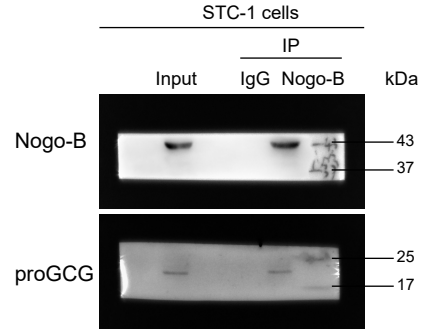

Figure 4f:

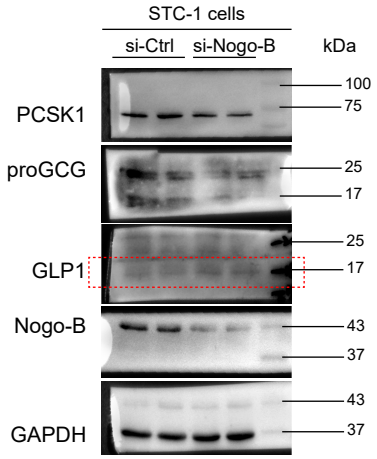

Supplementary Figure 1a:

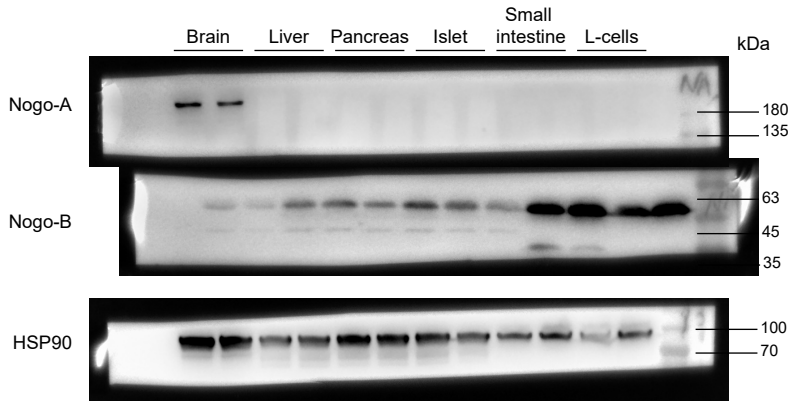

Supplementary Figure 1b:

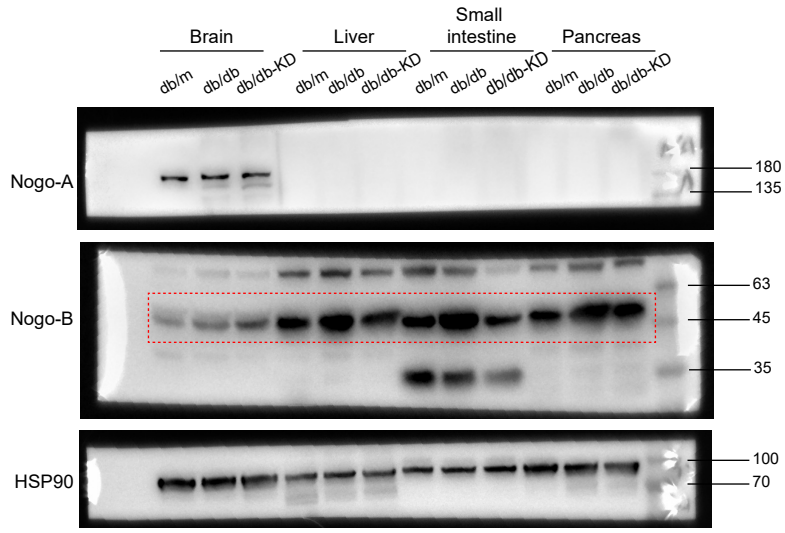

Supplementary Figure 2b:

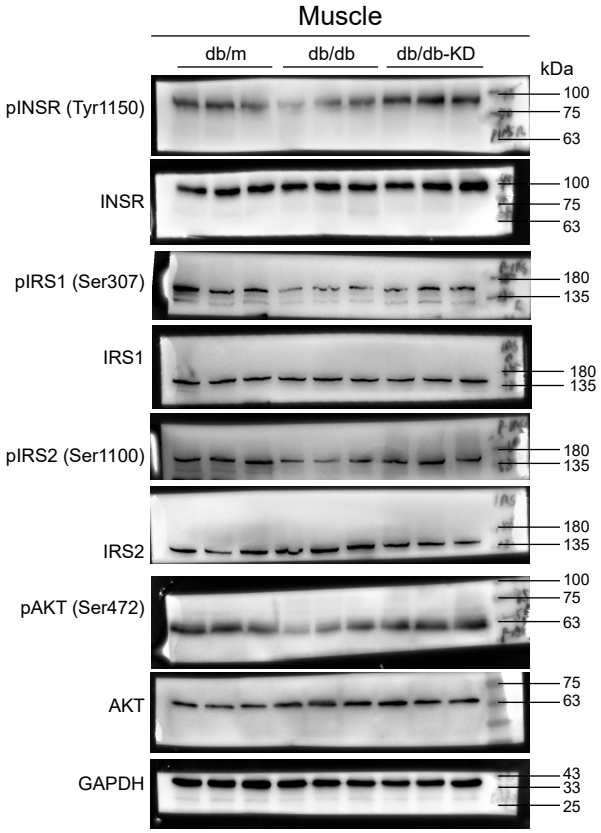

Supplementary Figure 4a:

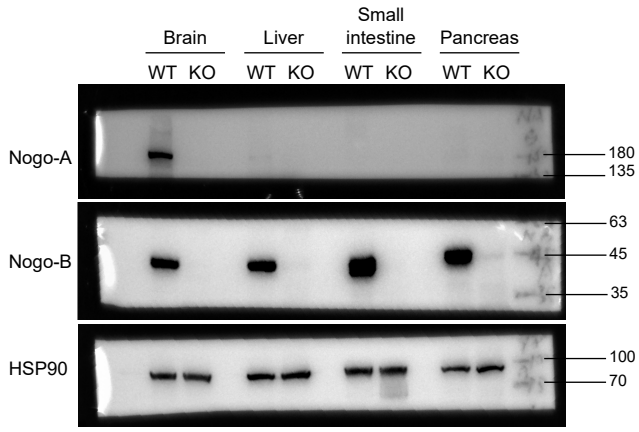

Supplementary Figure 5b:

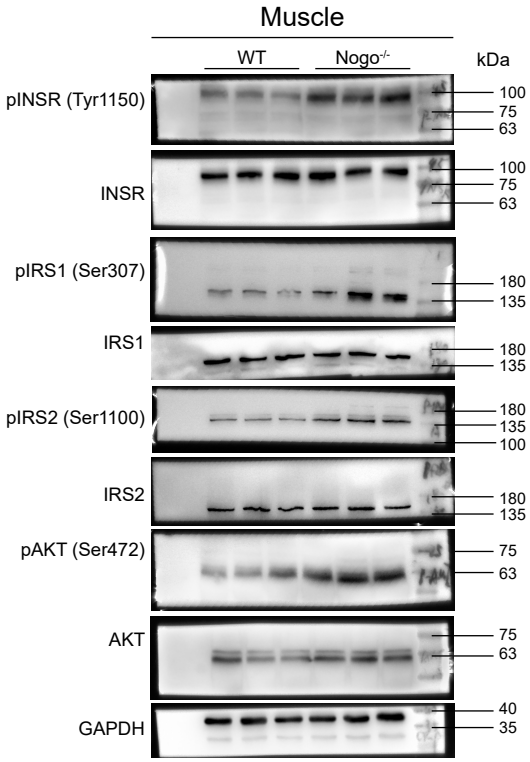

Supplementary Figure 7b:

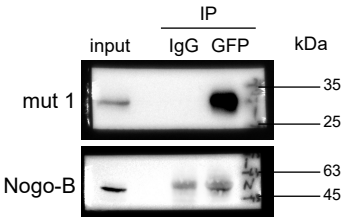

Supplementary Figure 7c:

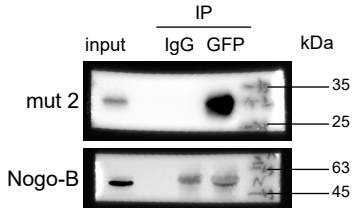

Supplementary Figure 7d:

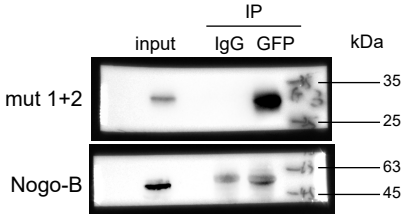

Supplementary Figure 7e:

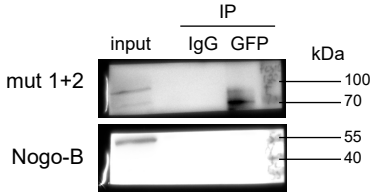

Supplementary Figure 8b:

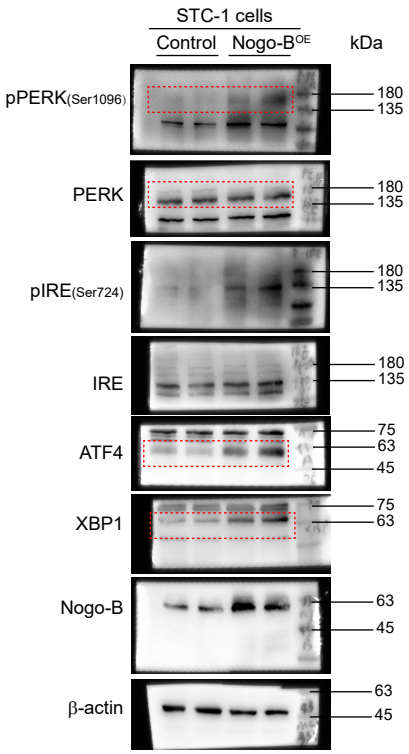

Supplementary Figure 8d:

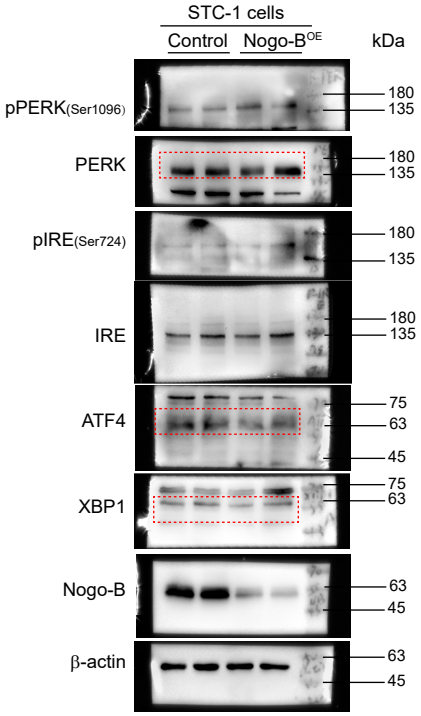

Supplementary Figure 9b:

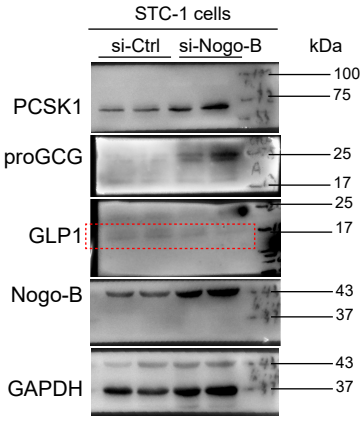

Supplementary Figure 11b:

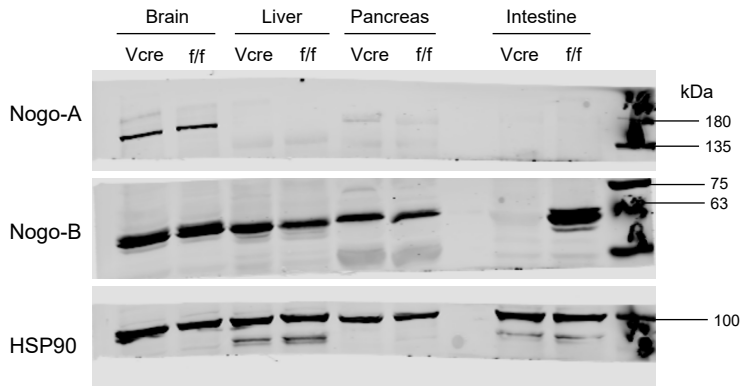

Supplementary Figure 11f:

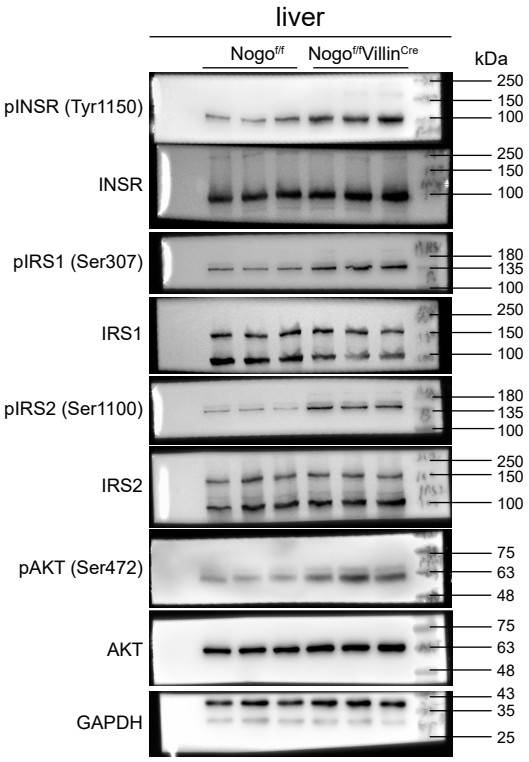

Supplementary Figure 11h:

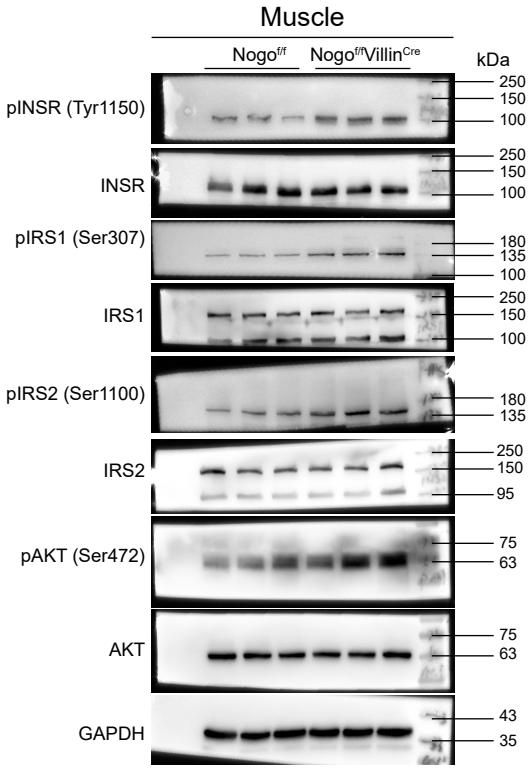

Supplementary Figure 13a:

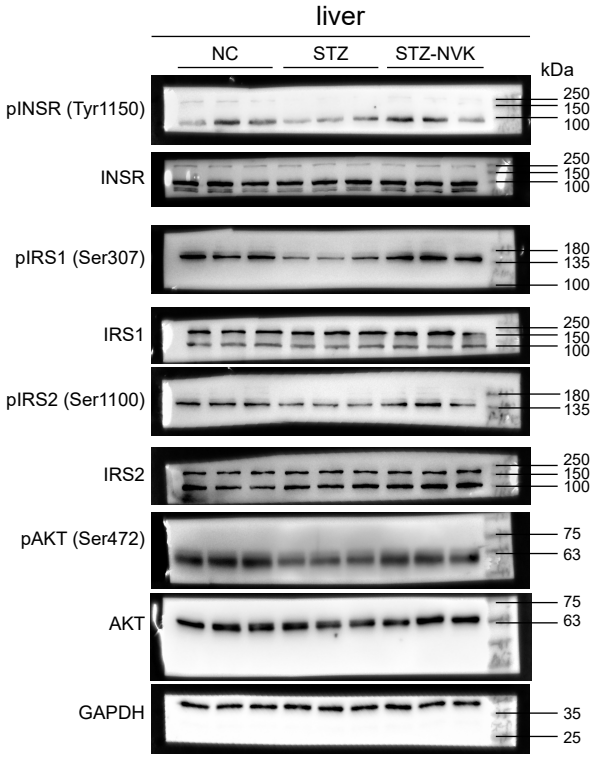

Supplementary Figure 13c: